International Research Journal of Innovations in Engineering and Technology (IRJIET)

ISSN (online): 2581-3048

Volume 6, Issue 4, pp 86-93, April-2022

https://doi.org/10.47001/IRJIET/2022.604018

Experimental and Analytical Study of Built Up section of Cold Formed Steel (CFS) by Bolted Connection

P.Pavatharini

Department of Civil Engineering, Parisutham Institute of Technology Sciences, Thanjavur, Tamilnadu, India

***Abstract* - This paper involves the experimental and analytical study of flexural strength of Cold Formed Steel (CFS) sections by using bolted connection. The analytical investigation of the built up section was carried out using finite element analysis software ABAQUS (Standard version 6.10) with 4 number of built up sections. The specimens consists of beams made of one or more Cold-Formed Steel (CFS) profiles namely, C (lipped channel) profiles and U (channel without lip) profiles, whereas the channel sections are connected along the flanges with bolts (M10). The experimental investigation shows the bending strength and behavior of CF built-up sections where, Four models are created in two groups, the first group of two specimens with 2mm thickness and second group of two specimens with 3.15mm thickness with varying web and flange dimensions taken from IS 811-1987. They are analyzed under two point loading conditions. The result shows the modes of buckling failure, their influence on the bending strength and behaviour of CF built-up sections. The influence of the height, thickness and span of the beams was studied and then experimental results are compared with the analytical results.**

Keywords: Flexural Strength, Channel section with and without lipped, Built up section.

I. INTRODUCTION

Cold-Formed Steel (CFS) is fabricated by a cold forming process where they are produced by sheet steel using stamping, rolling or presses in order to get a desired product. Experiments and research work were saying that it‘s had more advantage than hot-rolled steel, its provide economic structure. Cold-Formed Steel members are have been widely used in building constructions, bridge constructions, storage racks, grain bins, car bodies, railway coaches, transmission towers, transmission poles, drainage. Facilities and cold-Formed Steel products can be classified into three categories, members, panels, prefabricated assemblies. Cold-Formed Steel research and products, including codes and standards developed that are spearheaded by the American Iron and Steel Institute (AISI).

These buckling modes are mostly responsible for the ultimate strength of the compression members as they may occur even before parts of the cross-section yield. The low torsional stiffness, the high slenderness and the geometric imperfections that are characteristic of CFS members are some of the main causes for their high susceptibility to buckling.

II. ANALYTICAL INVESTIGATION

The finite element analysis software ABAQUS is a computational tool for modelling structures (ABAQUS/ Standard version 6.10). It is highly used to simulate the model under displacement control. It mainly helps to find ultimate load, stress criteria, displacement criteria, behavior of model failure mode and other useful values like support reaction etc.

A) Modeling Parameter

The specimens consisted of beams made of one or more cold- formed steel profiles, namely, C (lipped channel) and U (channel) profiles. Whereas the compound R-beams consisted of one C-profile and one U-profile connected in the flanges and connections are made with bolts. The Fig. 1 shows the cross-sectional view of CFS beams for bending test.

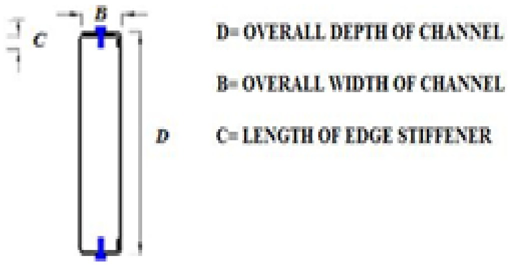

Figure 1: Cross Sectional View of CFS R-Beam

B) Section Property

Table 1 shows the sections, details for the cold-Formed steel R- cross sections, beams with 2 and 3.15 mm thickness. Cold-formed steel members are usually classified as channel sections, according to IS: 811-1987. Here C profile refers to the channel section with lipped and U profile refers to the channel section without lipped section. The span of the beam is taken as 1000mm with the Pitch and Edge distance of 60 mm and 50 mm respectively.

International Research Journal of Innovations in Engineering and Technology (IRJIET)

ISSN (online): 2581-3048

Volume 6, Issue 4, pp 86-93, April-2022

https://doi.org/10.47001/IRJIET/2022.604018

Table 1: Sections details for the CFS Beam

S. NO	Profile name	C Profile			U profile		R	T
		D	B	C	D	B		
1.	FE-R_1	70	40	15	74	40	3	2
2.	FE-R_2	80	50	15	84	50		
3.	FE-R_3	100	40	20	106.3	40	4.73	3.15
4.	FE-R_4	120	50	20	126.3	50		

Where,

R = Inside Radius (mm)

T = Thickness of CFS (mm)

C) Element Type

All the models were created by using shell elements (S4R) for the profiles and solid elements (C3D8R) for the bolts. The S4R element was chosen because it is a general-purpose shell element from the ABAQUS program library, which also takes transverse shear deformation into account as well as the thick shell elements.

The S4R element is double-curved, a four-node (4), quadrilateral and stress/displacement shell element (S) with reduced integration (R), a large-strain formulation, hourglass control and a first-order (linear) interpolation. Reduced integration elements converge non-monotonically and due to this reduced number of integration points hour glassing can occur in the S4R element, so an hourglass stabilization control feature is built into the element to suppress spurious modes. The reduced integration method reduces the processing time for model analysis. Each node has three displacements and three rotational degrees of freedom. Finally, all the six degrees of freedom from an independent bilinear interpolation function.

The C3D8R element is defined as a three-dimensional (3D), continuum (C), hexahedral and an eight-node brick element with reduced integration (R), hourglass control and first-order interpolation. These finite elements have three degrees of freedom per node, corresponding to translations in the three directions X, Y and Z (global coordinates).

D) Material Properties

Material non-linearity in the specimens was modeled with von Mises yield criterion and isotropic hardening. The stress–strain relationship of cold-formed steel profiles was described by a gradual yielding behavior followed by a considerable period of strain hardening. Fig. 2 shows the stress–strain curves used in the FEA for the CFS profiles based on tensile coupon test results. Where the apparent yield stress in the corners is increased was ignored.

Yield strength (F_y)	250 MPa
Young's Modulus (E)	210 GPa
Tensile Strength (F_u)	345 MPa
Poisson's Ratio (μ)	0.3

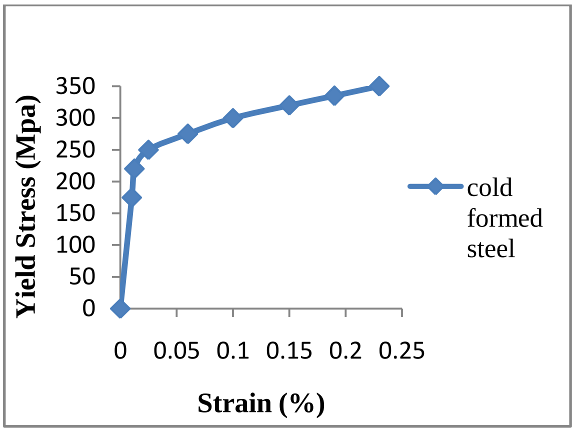

Figure 2: Stress - strain relationship of the CFS beam

E) Loading and Support Conditions

A three-dimensional computational model was used to simulate. The cross-sections of the different beam, support system and the beam loading system were reproduced with great accuracy in the numerical simulations. Therefore, with regard to the two-point loading on the beams, concentrated forces with the direction-Y were applied one third of the span from support at a distance of 333 mm. Fig. 3 shows the forces were applied at one-third of the span.

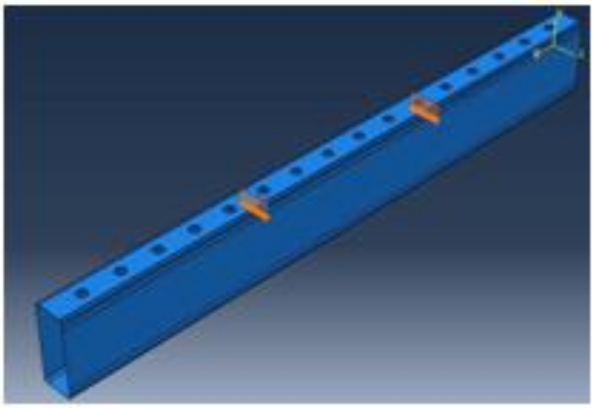

Figure 3: Load provided at one-third span of the beam

To simulate the pinned support, all degrees of freedom of the nodes located at the end of the beam were constrained. All simulated beams were modeled using the Centre line dimensions. Since the boundary conditions in the ABAQUS/Standard were used as U_1=0 and U_2=0. Fig. 4 shows a boundary condition was provided at the end side of the beam.

ISSN (online): 2581-3048
Volume 6, Issue 4, pp 86-93, April-2022
https://doi.org/10.47001/IRJIET/2022.604018

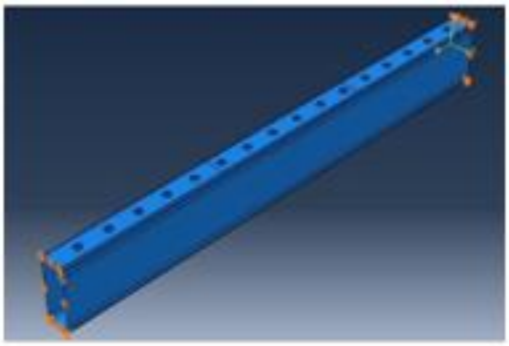

Figure 4: Boundary Conditions of R-Beam

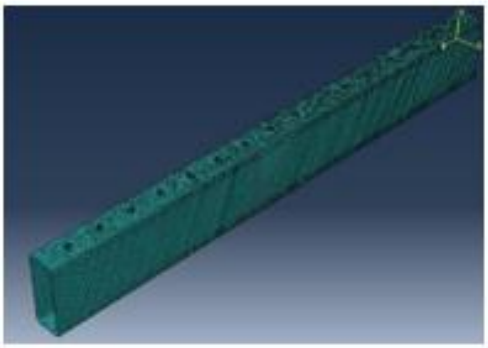

Figure 6: Meshing of R-Sections

F) Interaction

In the ABAQUS/Standard two assumptions were introduced in these analyses for modelling the contact behavior between the profiles and also between them and the bolt connections. As per IS 800-2007 the pitch and edge distance was chosen.

i. A tangential friction coefficient of 0.2 was assumed,
ii. A hard contact between the profile surfaces and a rough and hard contact was considered between the profiles and the bolt. Fig. 5 shows Interaction and bolt connection arrangement of sections.

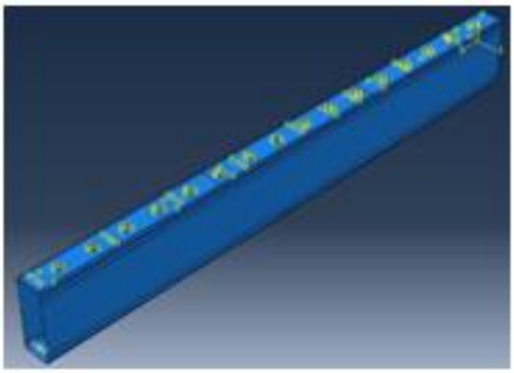

Figure 5: Connection Interaction of R-sections with bolts

G) Meshing

The influence of the finite element size on the behavior of cold-formed steel beams was studied. It was found that good simulation results could be obtained by using finite element meshes of 5x 5 for R-beams and mesh were automatically generated by the ABAQUS/ Standard version 6.10 program and used in all simulations Fig. 6 shows meshing pattern of the model, Meshing is used for accurate presentation of complex geometry, easy representation of the total solution, and capture of local effects. According to results requirement meshing can be increased (or) decrease.

H. Analytical Procedure

Then, a general geometrical and material nonlinear static analysis with imperfections (GMNIA) was undertaken with the purpose of simulating the structural behavior of cold-formed steel beams under bending at ambient temperature. The non-linear geometric parameter (*NLGEOM=ON) was set to deal with the geometric nonlinear analysis, namely, with the large displacement analysis, and Vertical displacements were also monitored at mid-span for the purposes of obtaining load– deflection graph. The parameters used in the nonlinear static analyses were:

- Maximum number of load increments = 100.
- Initial increment size = 0.1.
- Minimum increment size = 0.000001.
- Automatic increment reduction enabled, and large displacements enabled.

III. ANALYTICAL RESULTS

It was observed from analytical investigations that occurred under the loading point of the Y-directions. Were failure mode was occurred at both web and flange. It is highly used to simulate the model under displacement control. It mainly helps to find ultimate load and the behavior of model failure mode, stress criteria, displacement criteria and other useful values like the support reaction the maximum deflections, ultimate load value, buckling modes for the various sections as follows:

Displacement Behaviour

In all computational models the failure mode, ultimate load carrying and maximum displacement are predicted. Here two-point load was punched by loading beam at one-third length of beam. Due to the punching effect at one third span buckling occurred on the outer most web part. It means distortional buckling occurred at built-up sections. The load–displacement curves for the tested cold-formed steel beams as a function of the vertical displacement at section.

International Research Journal of Innovations in Engineering and Technology (IRJIET)

ISSN (online): 2581-3048

Volume 6, Issue 4, pp 86-93, April-2022

https://doi.org/10.47001/IRJIET/2022.604018

Fig. 7, 8, 9, 10 shows the analytical behavior of FE-R1 where they are stimulated by the procedure given above.

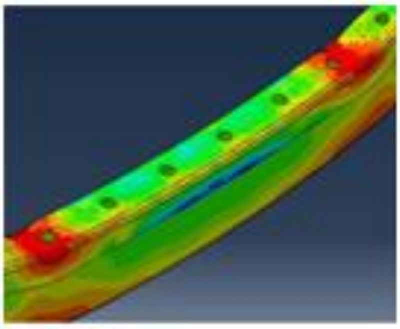

Figure 7: Buckling behavior of beam (FE-R_1)

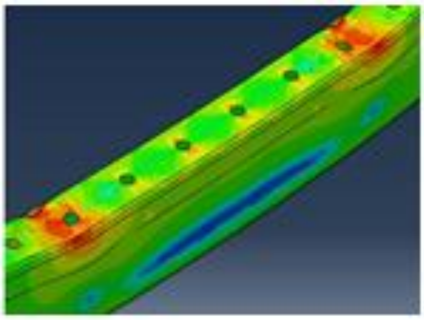

Figure 8: Buckling behavior of beam (FE-R_2)

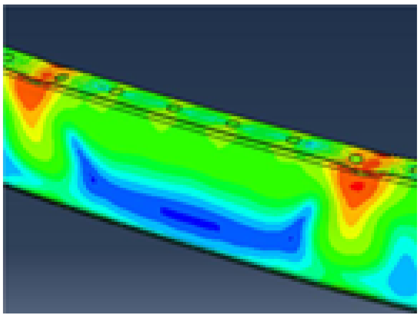

Figure 9: Buckling behavior of beam (FE-R_3)

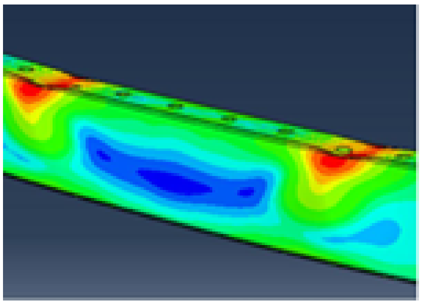

Figure 10: Buckling behavior of beam (FE-R_4)

Table 2 shows the maximum ultimate load, displacement and analytical bucking behavior of CFS beam FE-R_1, FE-R_2, FE-R_3, FE-R_4.

Table 2: Analytical behavior of CFS Beam

S. no	PROFILE NAME	Ultimate Load (kN)	Maximum Deflectio (mm)	Buckling Modes
1.	FE-R_1	27.83	16.20	Distortional buckling
2.	FE-R_2	33.04	12.60	
3.	FE-R_3	66.83	10.84	
4.	FE-R_4	71.06	7.84	

Fig. 11, 12, shows the load versus displacement graph for the beam FE-R_1, FE-R_2.In the graph (A-B) is the elastic zone were load is proportional to displacement and the point (B-C) is the plastic zone. The point (C) represents ultimate load and corresponding displacement value.

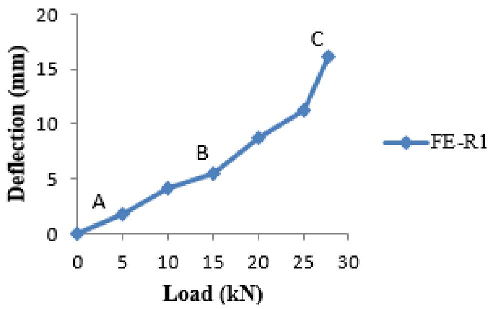

Figure 11: Load (Vs) Displacement (FE-R_1)

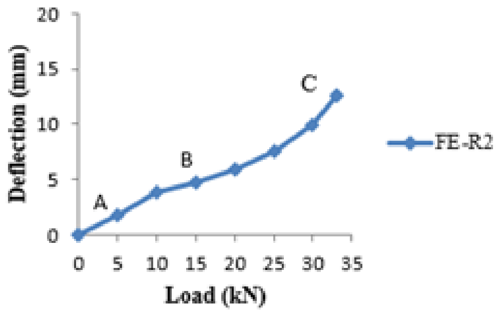

Figure 12: Load (Vs) Displacement (FE-R_2)

IV. EXPERIMENTAL INVESTIGATION

Computerized universal testing machine is used for doing experimental investigation in order to find the maximum ultimate load carrying capacity, the maximum displacement of the specimen and calibrate load v/s displacement graph, Here UTM was used as two- bending test for experimental investigation.

A) Test Specimens

The specimens consisted of beams made of one or more cold- formed steel profiles, namely, C (lipped channel) and U (channel without lip) profiles. All these profiles had the nominal thickness 2 mm, and inside radius 3 mm. The edge

ISSN (online): 2581-3048
Volume 6, Issue 4, pp 86-93, April-2022
https://doi.org/10.47001/IRJIET/2022.604018

stiffeners of the C- profiles were 15mm long and the nominal flange width varied from 40 and 60 mm, for the C-profiles and U-profiles also the nominal web depth varied from 70, 80, 100, and 120 mm for the C and U-profiles constantly, it was fixed as the span of the beam was 1000 mm and connections are made by bolts M10. As per IS 800-2007 the pitch and edge distance as 60, and 50mm respectively. Experimental section details of the cold formed steel beam with built-up sections as shows in Table 3.

Table 3: Experimental section details of the CFS Beam

S. No	Profile name	C profile			U profile		R	T
		D	B	C	D	B		
1.	FE-R_1	70	40	15	74	40	3	2
2.	FE-R_2	80	50	15	84	50		
3.	FE-R_3	100	40	20	106.3	40	4.73	3.15
4.	FE-R_4	120	50	20	126.3	50		

B) Test Set Up

Schematic and overall views of the experimental system used in the quasi-static bending tests are shown in Fig. 13 and 14 respectively. As it can be seen in Fig. 13, the test specimens were loaded at two points 333.33mm (one-third of the beam span) from the supports of the beam in such a way that between the two loading points the beam was under pure bending state. The loading was applied by a UTM (universal testing machine).

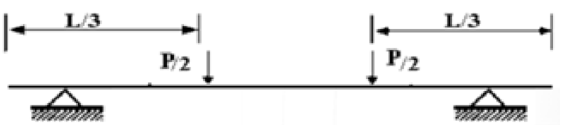

Figure 13: Schematic view of the experimental set-up

Figure 14: Overall view of the experimental set-up

C) Test Procedure

Two-point bending tests were used to assess the ultimate bending strength of the cold formed steel beams. These experiments provided useful results for detailed numerical studies. The load was applied under displacement control at a rate of 0.01 mm/s to the specimen failed and reached its unloading stage, where the beam deformation or the lateral rotation of the beam was too large, or the maximum load was reached. Therefore, dial gauge was used to measure the vertical displacements of the beams at mid sections. A number of strain gauges were also placed around the beam to measure the longitudinal strains

D) Experimental Results

In all the experimental specimens the failure mode, ultimate load carrying and maximum displacement are predicted. Here two-point load was punched by loading beam at one-third length of span. Due to the punching effect at one third span bulging occurred at outer most web part of U-sections. It means distortional buckling occurred at R-sections. It shows the results of tests carried out for all R- type of beam. Fig. 15, 16, 17 and 18 are showing the experimental displacement and buckling behavior of beams of B-R_1, B-R_2, B-R_3, B-R_4.

Figure 15: Buckling behavior for (B-R_1)

Figure 16: Buckling behavior for (B-R_2)

Figure 17: Buckling behavior for (B-R_3)

International Research Journal of Innovations in Engineering and Technology (IRJIET)

ISSN (online): 2581-3048

Volume 6, Issue 4, pp 86-93, April-2022

https://doi.org/10.47001/IRJIET/2022.604018

Figure 18: Buckling behavior for (B-R_4)

Table 4 shows the maximum ultimate load; displacement and experimental buckling behavior of CFS beam B-R_1.

Table 4: Experimental behavior of CFS Beam

S. no	PROFILE NAME	Ultimate Load	Maximum Deflection	Buckling Modes
1.	FE-R_1	31.40	14.44	Distortional buckling
2.	FE-R_2	36.75	12.00	
3.	FE-R_3	69.80	9.21	
4.	FE-R_4	72.20	6.82	

Fig. 19 shows the load versus displacement graph for the beam B-R1 in the experimental investigation. In the graph (A-B) is the elastic zone were load is proportional to displacement and the point (B-C) is the plastic zone. The point (C) represents ultimate load and corresponding displacement value.

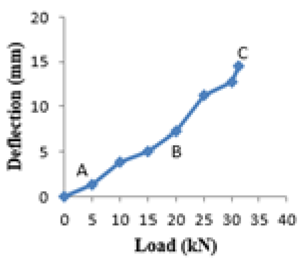

Figure 19: B-R_1

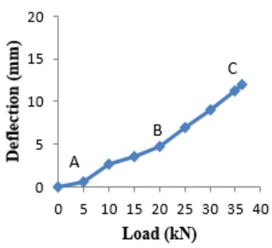

Figure 20: B-R_2

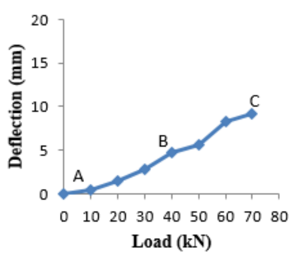

Figure 21: B-R_1

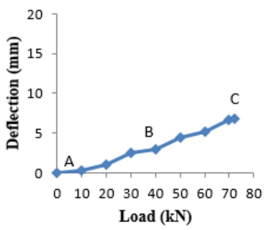

Figure 22: B-R_1

V. RESULTS AND DISCUSSIONS

The beam model was created in ABAQUS is expected to have an acceptable level of accuracy and coincides with experimental results. The comparison of maximum deflections, ultimate load value, buckling modes for the various sections in analytical and experimental was followed:

A) Load Carrying Capacity

All curves from FEA fit closely with the experimental curves. This good agreement and accuracy between the experimental and numerical results ensures a strong validity of the developed finite element model. From these graphs B-R1, B-R2, B-R3 and B-R4 indicate experimentally it can be seen that the maximum ultimate load of 31.4, 36.75, 37.15 and 38.43 kN respectively. Also, it's that the maximum load carrying of the beams B-R1, B-R2, B-R3, and B-R4 in the analytical investigation was,27.83, 33.04, 66.83, 71.06 kN respectively.

B) Failure Modes

It was noticed that the R beams started to buckle as distortional buckling occurred on the most affected U buckling had after the failure of (U profile) web portions. The distortional buckling always occurred nearer to the roller support of the beams rather than in mid-span of the beam.

The distortion buckling modes that were responsible for the collapse of the beams are clearly identified. In the numerical simulations, and experimental study of the structural behavior of CFS beams, B-R1, B-R2, B-R3, and B-R4 different sections that was changed in the Height and Width were shown in the below table.

Table 5: % variation of ultimate load

S. No	Name	Ultimate Load (kN)		% in Variation
		EXP	FEM	
1	B-R1	31.40	27.8	11.46
2	B-R2	36.75	33.04	10.09
3	B-R3	69.80	66.83	4.25
4	B-R4	72.20	71.06	1.57

Table 6: % variation of ultimate load

S. No	Name	Maximum Deflection (mm)		% in Variation
		EXP	FEM	
1	B-R1	14.44	16.20	12.18
2	B-R2	12.00	12.60	5.00
3	B-R3	9.21	10.84	17.69
4	B-R4	6.82	7.84	14.9

ISSN (online): 2581-3048
Volume 6, Issue 4, pp 86-93, April-2022
https://doi.org/10.47001/IRJIET/2022.604018

The comparison of numerical failure load and the experimental failure load of the tested specimens under bending as shown in Fig. 23, 24, 25, 26. The results of load versus displacement obtained from experimental work were slightly varied from analytical work. The difference in the analytical and experimental investigation of ultimate load carrying capacity and the deflection were mentioned in the table.

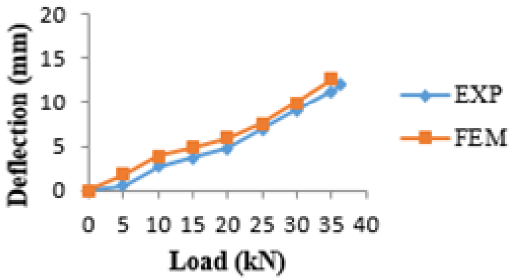

Figure 23: Comparison of Results for beam (B-R_1)

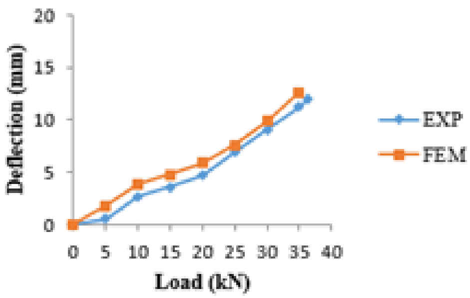

Figure 24: Comparison of Results for beam (B-R_2)

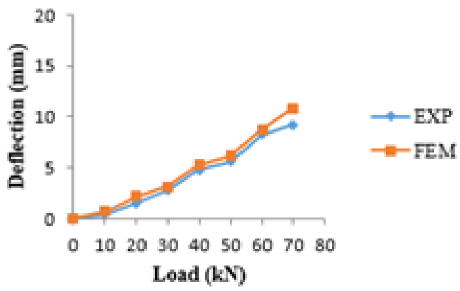

Figure 25: Comparisons of Results for beam (B-R_3)

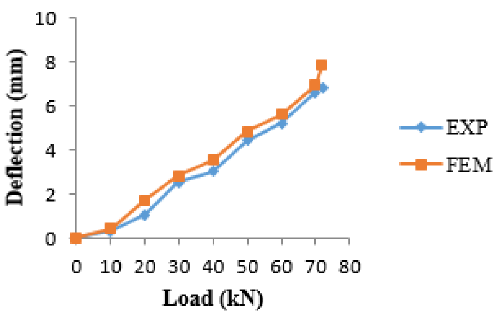

Figure 26: Comparisons of Results for beam (B-R_4)

VI. CONCLUSIONS

An experimental and numerical investigation into the behavior of cold-formed steel, R-beams under bending conditions were carried out for four different specimens. The failure mode obtained from analytical study is a distortion buckling and it is found to be the same from experiment study. The difference in ultimate load carrying capacity is being varied 11.3%, 10.09%, 4.25%, and 1.57% for the beam B-R1, B-R2, B-R3, and B-R4.

In order to improve the structural behavior of these R-shaped cross sections of beams, the authors suggested, for instance, that the U profiles of these beams are replaced by lipped U profiles like the C profiles, but with the lips towards the exterior side of the profile. In other words, the U profiles should be replaced by hat (omega) profiles.

VII. SCOPE OF FUTURE STUDY

Hence, different innovations can be done by changing the parameter of the beam profile. It is recommended that further experimental and numerical research is needed to develop new design guidelines for lateral-torsional buckling of cold-formed steel beams comprised of more than one profile and connections.

REFERENCES

[1] Ajeet Sharma, et al (2016), "Experimental Study on the Flexural-Torsional Behavior of Cold-Formed Steel Channel Section Connected Back to Back".

[2] Ashok M, Jayabalan P, Jaya Prabakaran K, (2016), "Flexural Behaviour of Cold Formed Steel Hat Shaped Beams".

[3] Abhijith V J, et al (2015), "Web buckling Analysis of lipped and hollow flanged light gauge sections with web hole".

[4] Beulah GnanaAnanthi G, (2015), "Numerical and Theoretical Studies on Cold-Formed Steel unlipped Channels Subjected to Axial Compression".

[5] Ben Young, Gregory J. Hancock. (2004), "Web crippling of cold-formed un-lipped channels with flanges restrained".

[6] Beale R.G, Godley M.H.R, Enjily V. (2001), "A theoretical and experimental investigation into cold-formed channel sections in bending with the unstiffened flanges in compression".

[7] Ben Young, Gregory J. Hancock. (2004), "Web crippling of cold-formed un-lipped channels with flanges restrained".

[8] Cao Hung Pham, Gregory J. Hancock. (2010), "Numerical simulations of high strength cold-formed purlins in combined bending and shear".

ISSN (online): 2581-3048
Volume 6, Issue 4, pp 86-93, April-2022
https://doi.org/10.47001/IRJIET/2022.604018

[9] Deepavani R, Chitra S, Dr.Sudha K, (2016), "Analytical Investigation on Cold Formed Steel Latticed Built-Up I Beam with lipped Angles under single point loading conditions".

[10] Fadhluhartini Muftah, et al (2014),"Ultinate Load of Built-Up Cold Formed Steel Column".

[11] Haimingwang, Yaochunzhang. (2009), "Experimental and numerical investigation on cold formed steel C-section flexural members".

[12] Kumaran V, Sureshbabu S, (2016), "Experimental Study on Torsional Behaviour of Light gauge Steel".

[13] Landolfo R, Mammana O, PortioliF, Di Lorenzo G, Guerrieri M.R. (2008), "Laser welded built-up cold-formed steel beams Experimental investigations".

[14] Lei Xu,Papia Sultana, Xuhong Zhou. (2009), "Flexural strength of cold-formed steel built-up box section".

[15] Luis Laim,joaopaulo C. Rodrigues,LuisSimoes da silva,(2013),"Experimental and numerical analysis on the structural behavior of cold-formed steel beams".

[16] Madulat S, Bambach M R, Zhao X.L. (2012), "Inelastic behavior and design of cold-formed channel section in bending".

[17] Mohamed arshath S, Kanaga A, Dr.G.Vani(2016), "Experimental Study on Flexural Behavior of Cold Formed Hat section subjected to Two Point Loading".

[18] Portioli F, et al (2016), "Contact buckling effects in built-up cold formed steel beams".

[19] Pradeep T, Arun N, (2015), "Numerical Optimization of Cold Formed Closed Built-up Steel Column".

[20] Prakash M. Mohite, Aakash C. Karoo, (2015), "Buckling Analysis of Cold Formed Steel for Beams".

[21] Parvati S Prakashet el, (2014), "Flexural Behavior of Cold Formed Steel Beams with end Stiffeners and Encased Web".

[22] Raghul V, Uma Maheswari N (2015), "Analytical Investigation on Cold- Formed Steel Built-Up Section under Flexure".

[23] Sudha K, Sukumar S, (2014), "Behaviour of Cold-Formed Steel Built-up I Section Under Bending.

[24] Karthika R, (2016), "Failure modes of Cold formed steel beam- A Review".

[25] IS: 800 (2007) "General Construction in Steel- Code of Practice".

[26] IS 801 (1975) "Code of practice for use of cold-formed light gauge steel structural members in general building construction".

[27] IS: 811 (1987) "Specification for Cold Formed Light Gauge Structural Steel sections".

Citation of this Article:

P.Pavatharini, "Experimental and Analytical Study of Built Up section of Cold Formed Steel (CFS) by Bolted Connection" Published in *International Research Journal of Innovations in Engineering and Technology - IRJIET*, Volume 6, Issue 4, pp 86-93, April 2022. Article DOI https://doi.org/10.47001/IRJIET/2022.604018

****